Position-dependent linkages of fibronectin–integrin–cytoskeleton

Takayuki Nishizaka*†‡, Qing Shi*, and Michael P. Sheetz*§

*Department of Cell Biology, Duke University Medical Center, Durham, NC 27710; and †Department of Physics, School of Science and Engineering, Waseda University, 3-4-1 Okubo, Shinjuku-ku, Tokyo169-8555, Japan

Edited by Thomas D. Pollard, The Salk Institute for Biological Studies, La Jolla, CA, and approved November 1, 1999 (received for review February 24, 1999)

Position-dependent cycling of integrin interactions with both the cytoskeleton and extracellular matrix (ECM) is essential for cell spreading, migration, and wound healing. Whether there are regional changes in integrin concentration, ligand affinity or cytoskeleton crosslinking of liganded integrins has been unclear. Here, we directly demonstrate a position-dependent binding and release cycle of fibronectin–integrin–cytoskeleton interactions with preferential binding at the front of motile 3T3 fibroblasts and release at the endoplasm–ectoplasm boundary. Polystyrene beads coated with low concentrations of an integrin-binding fragment of fibronectin (fibronectin type III domains 7–10) were 3–4 times more likely to bind to integrins when placed within 0.5 microns vs. 0.5–3 microns from the leading edge. Integrins were not concentrated at the leading edge, nor did anti-integrin antibody-coated beads bind preferentially at the leading edge. However, diffusing liganded integrins attached to the cytoskeleton preferentially at the leading edge. Cytochalasin inhibited edge binding, which suggested that cytoskeleton binding to the integrins could alter the avidity for ligand beads. Further, at the ectoplasm–endoplasm boundary, the velocity of bead movement decreased, diffusive motion increased, and approximately one-third of the beads were released into the medium. We suggest that cytoskeleton linkage of liganded integrins stabilizes integrin-ECM bonds at the front whereas release of cytoskeleton-integrin links weakens integrin-ECM bonds at the back of lamellipodia.

Motility of adherent cells is critical for many biological functions such as wound healing, lymphocyte function, and development. Cells apply force to the matrix through the integrin-cytoskeleton linkage (1, 2), and the integrins appear to participate in multiple cycles of binding to and release from ECM in cell migration on specific substrata (3). Models of cell migration have described several steps in the process, including extension to new regions, attachment to extracellular matrix (ECM) (adhesion), force generation, and release from ECM to allow further movement and recycling (4). An additional requirement for directed migration is that there must be position dependence of attachment to and release from substrate-bound ECM.

ECM contacts are initiated at the newly extended edge of the cell because that is the first region to contact exposed ECM molecules. Experiments in fish keratocytes have shown that the leading edge is also the domain where crosslinked glycoproteins are rapidly attached to the cytoskeleton (5). An implication of those studies is that the edge region is specialized for the binding of cross-linked membrane glycoproteins to the cytoskeleton. One explanation for the attachment in that region is that membrane molecules involved in attachment are concentrated there. Indeed, integrins are concentrated at the leading edge of fish keratocytes (C. G. Galbraith and M.P.S., unpublished results). Alternatively, cytoskeletal attachment proteins are concentrated at the edge such as those which catalyze actin filament assembly in the keratocyte (6). Such edge specificity has not been reported for crosslinked integrin–cytoskeleton interactions related to cell migration.

Once the matrix has moved rearward, the integrin must release from the matrix molecule. Three possible mechanisms for integrin release from ECM-binding sites are mechanical release caused by high forces at the back of the cell (2, 7, 8), calpain-mediated enzymatic cleavage of integrin/cytoskeleton linkages (9, 10), or biochemical release. Phosphatase-dependent release has been suggested for vitronectin receptors, in the case of calcineurin-dependent $\alpha v\beta 3$ integrin release (11), but not for the major fibronectin-binding site, the $\alpha 5\beta 1$ integrin. A fourth mechanism could involve the loss of cytoskeletal attachment to the ECM-crosslinked integrins. Unbound integrins could then diffuse away from the ECM molecules before rebinding. Such an avidity mechanism would not necessarily involve alterations in integrin-ECM affinity but would rely primarily on position-dependent cytoskeleton assembly and disassembly (explained further in Fig. 5).

Here, we examined the position dependence of fibronectin bead binding and release by using optical tweezers manipulation on 3T3 cells. We found a strikingly narrow region of preferential binding at the leading edge that correlated with the region of increased attachment to the cytoskeleton. Release of fibronectin beads occurred preferentially at the ectoplasm–endoplasm boundary after apparent detachment from the cytoskeleton. Both observations are consistent with the hypothesis that the cytoskeleton binding of liganded integrins increases avidity of binding for multimeric ECM complexes.

Materials and Methods

Bead Preparation. The fragment of fibronectin (integrin-binding domain of fibronectin type III, FNIII7–10; ref. 12) was used to avoid an aggregation of ECM and beads. Carboxylated polystyrene (1 μm) beads (Polysciences, Warrington, PA) were precoated with the mixture of 97% native BSA (Sigma) and 3% biotinamidocaproyl-labeled BSA (biotinylated BSA; Sigma) using a standard procedure (13). Then 2 mg/ml Neutra Lite avidin (Molecular Probes) was added and incubated overnight on ice. The beads were washed and mixed with the complex of biotinylated BSA and biotinylated FNIII7–10 to avoid the local aggregation of ligand on single beads. We used biotinylated BSA:FNIII7–10 (1:1 in weight ratio) for all experiments, except 1:0 for the control experiment in Fig. 2*a*. Antibody for chicken $\beta 1$ integrin chain, biotinylated ES66 mAb (refs. 14 and 15), was used for the antibody-coated bead.

Cell Preparation and Experiments. NIH 3T3 mouse fibroblasts transfected with chick $\beta 1$ integrin (7, 14) were seeded on

This paper was submitted directly (Track II) to the PNAS office.

Abbreviations: ECM, extracellular matrix; FNIII7–10, fibronectin type III domains 7–10; RGD, Arg-Gly-Asp peptide.

‡Present address: Core Research for Evolutional Science and Technology (CREST) Genetic Programming Team 13, 907 Nogawa, Miyamae-ku, Kawasaki, Kanagawa 216-0001, Japan.

§To whom correspondence and reprint requests should be addressed. E-mail m.sheetz@cellbio.duke.edu.

The publication costs of this article were defrayed in part by page charge payment. This article must therefore be hereby marked "*advertisement*" in accordance with 18 U.S.C. §1734 solely to indicate this fact.

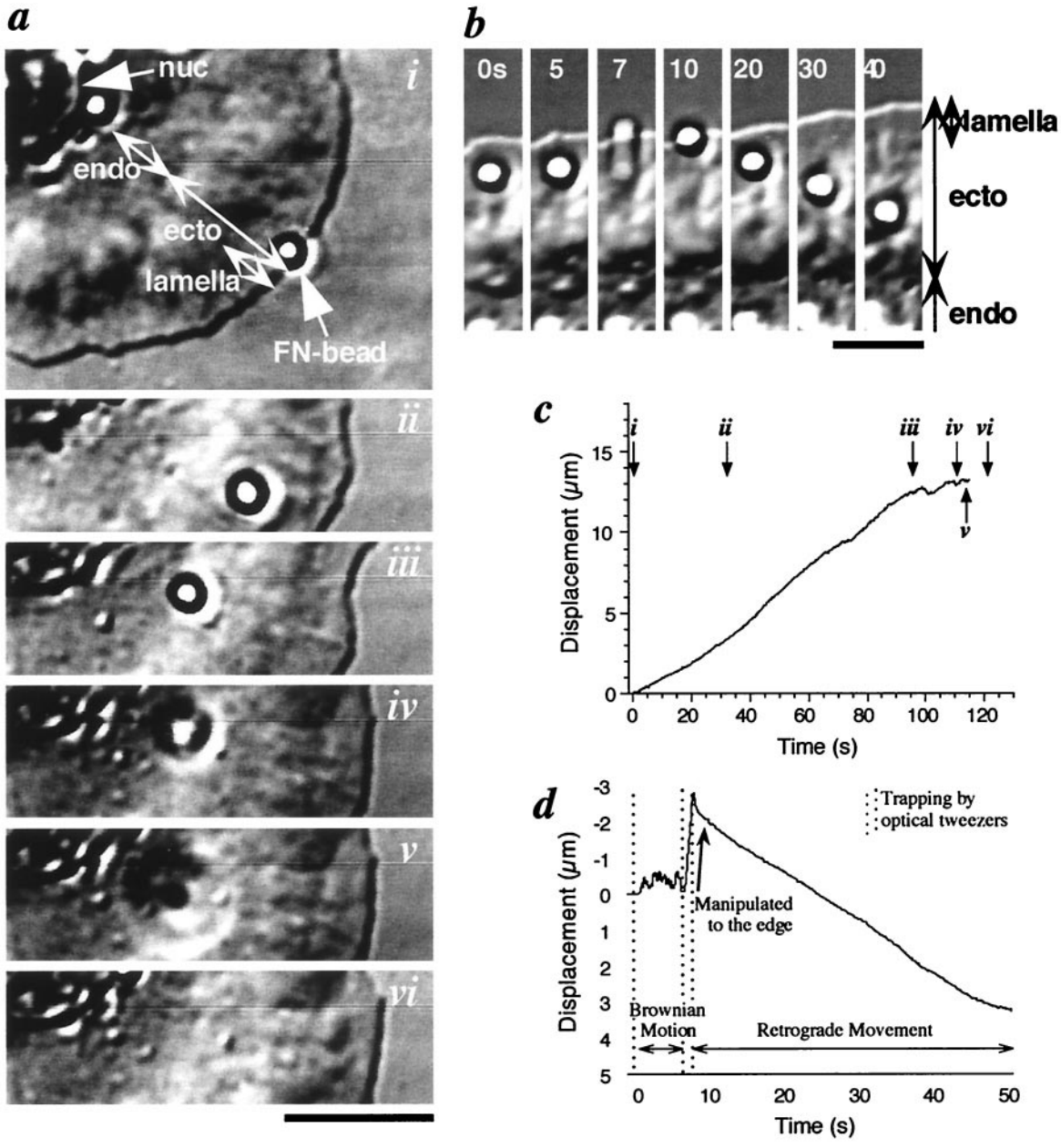

Fig. 1. Behavior of a bead coated with a low concentration of FNIII7–10. (*a*) Video-enhanced differential interference contrast micrographs show binding and release of a FNIII7–10 bead. The bead was carried to the edge of the lamellipodium with an optical tweezers and released from the trap (*i*). It immediately moved retrogradely across the lamellipodium (*ii*), and the velocity decreased at the boundary between ectoplasm and endoplasm (*iii*). The bead then detached from the cell surface (*iv*) and diffused out of focus into the medium (*v* and *vi*). (*b*) Video micrographs show attachment of diffusing bead and rearward movement after being brought to edge. (*c*) The trajectory of the bead along the direction of the displacement in *a*. *i–vi* Correspond to the micrographs in *a*. (*d*) The bead trajectory of *b*. [Scale bars, 10 μm (*a*) and 5 μm (*b*)]. Nuc, nuclear; endo, endoplasm; ecto, ectoplasm; and lamella, lamellipodium.

laminin-coated coverslips after trypsin treatment (1, 14, 16). DMEM with 10% serum (GIBCO/BRL) and Hanks' balanced salt solution with 1 mM Ca^{2+} were used as media for standard experiments and the Mn^{2+} experiment (Fig. 2*d*), respectively. After >4 h at 37°C, we chose trigonal cells with an actively spreading lamellipodium (7, 14) and checked the edge specificity with 7–47 beads on each cell in Fig. 2*a*. For the Arg-Gly-Asp peptide (RGD) experiment (Fig. 2*c*), Gly-Arg-Gly-Asp-Ser (GRGDS) peptide (Sigma) was used. For the fluorescence analysis cells were fixed with 4% paraformaldehyde for 10 min, washed three times, and then exposed to the medium containing 20 μg/ml biotinylated FNIII7–10 and 5 mg/ml BSA for 1 hr. Cells were fixed again, and finally, a rhodamine antibody for biotin (Sigma) was infused. Control experiments were performed in the presence of 1 mg/ml GRGDS peptide in FNIII7–10 treatment procedure.

Optical Tweezers System and Data Analysis. We used the same optical tweezers system as described before (1) except that it was equipped with a movable mirror with dc servomotors (optmike-e; Sigma Koki, Hidaka, Japan) for moving the trap center at a constant rate (Fig. 1 *b* and *d*). The bead was trapped with 3.7–4.9 mW of laser power after the objective, which produced a maximal force of ≈5 pN for displacements in the xy-direction (1). High laser powers caused nonspecific cytoskeletal attach-

ment of BSA beads. The probability of the cytoskeletal attachment increased with the laser power, and finally all of the beads showed retrograde movement after being pushed into the cell membrane for 3 s with 60 mW of laser power (data are not shown). The position of the bead on the cell surface was determined with nanometer precision (17, 18). The velocity of forward and of retrograde movements were determined from the displacement of the nucleus for 30–140 s and from the linear portion of the track of the bead on the ectoplasm (e.g., 0–90 s in Fig. 1*c*), respectively. In Fig. 4*a*, the one exceptional bead that detached at 20 μm was neglected in calculating the correlation coefficient.

Bead Attachments. Beads were trapped in the medium, manipulated to a cell surface, held there for 2.5–3.5 s, and then released. The bead behavior after release from the tweezers was classified in four ways: unattached, indirectly attached, membrane attached, and cytoskeletally attached (retrograde movement) (14). To confirm whether the bead was "indirectly attached" or "membrane attached," we retrapped all beads showing two-dimensional Brownian motion on a cell surface and tried to move them off the cell edge. Beads attached directly to a membrane protein always stopped at the edge of a cell, whereas beads attached to the membrane indirectly through a fibrous component went beyond the cell edge and on release diffused toward the cell center. When we used 1-μm diameter beads coated with BSA as the control experiment for ligand-coated beads, ≈50% of the beads were indirectly attached. Thus, we judged that the beads that were indirectly attached were nonspecifically bound and grouped the beads that were indirectly attached and "unattached" in the same class, "no membrane attachment" in the histograms of Figs. 2 and 3.

Definition of Terms. Ectoplasm is defined as the thin, rigid structure in the front part of the cell, which is rich in actin and depleted of membranous vesicles. Endoplasm is defined as the region just behind ectoplasm where movements of many membranous vesicles were observed. The boundary between them is often structurally visible as in Fig. 1 *a* and *b* and functionally clear because the release of fibronectin beads preferentially occurred there (see *Results*, *Discussion*, and Fig. 4).

Results

Position Dependence of Fibronectin-Coated Bead Binding. Fig. 1*a* shows a typical example of cytoskeletal attachment of a bead coated with a low concentration of FNIII7–10. The bead immediately showed steady directed movement on the dorsal surface of the cell (*i–iii*), i. e., retrograde movement, after turning off the trap (1, 16). Although the majority of the beads that bound to the membrane moved rearward (82%), some beads showed two-dimensional Brownian motion on the cell surface instead of retrograde movement (0–6 s in Fig. 1*b*). When we recaptured diffusing beads, brought them to the edge (7 s in Fig. 1*b*), and released them, the Brownian motion did not resume but retrograde movement immediately started (10–40 s in Fig. 1*b*).

Fig. 1 *c* and *d* show the trajectories of the bead in Fig. 1 *a* and *b*, respectively. Beads move steadily rearward in *i–iii* in Fig. 1*c*, and for 8–50 s in Fig. 1*d* beads show retrograde flow from the edge of the cell toward the nucleus ($1.2 \pm 0.3 \times 10^{-1}$ μm/s, n = 12). The beads moved with the same speed as small structures on the cell surface, suggesting retrograde movement of the bead relates to the flow of cytoskeletal structures in ectoplasm. Note that these rearward movements are measured relative to the substratum. In other words, data do not include the relatively slow forward movement of each cell body ($2.2 \pm 0.7 \times 10^{-2}$ μm/s, n = 10).

In Fig. 1 *b* and *d*, the Brownian motion changed to retrograde movement when the bead was moved to the edge ≈7 s. This result supported the hypothesis that attachment to the cytoskeleton and retrograde movement occurred preferentially at the edge of the cell (5). To quantify binding, we placed beads at various positions on the lamellipodium for 3 s using optical tweezers (see Fig. 2*a*). Within 0.5 μm of the edge, 63% of the beads bound and showed retrograde movement. In contrast, the cytoskeletally attached population decreased below 20% when beads were held >0.5 μm from the edge using the same trapping force and holding time. We also found that a fraction of cells that did not show the edge specificity (20%, 5 cells in 25). In these cells, the binding probability was above 60% at any position, independent of the distance from the edge (data from these cells are not included in Fig. 2). The shape of these cells was morphologically the same as the other cells that showed edge specificity, so that we could not determine the origin of this difference so far. It may relate to the motility state because cells that were not motile also did not have higher binding at the edge or rearward movement. In the majority of motile cell lamellipodia, fibronectin beads bound preferentially at the very leading edge.

To confirm that the cytoskeletal attachment of the beads was caused by the interaction between FNIII7–10 and integrin, we performed four different control experiments. First, we used

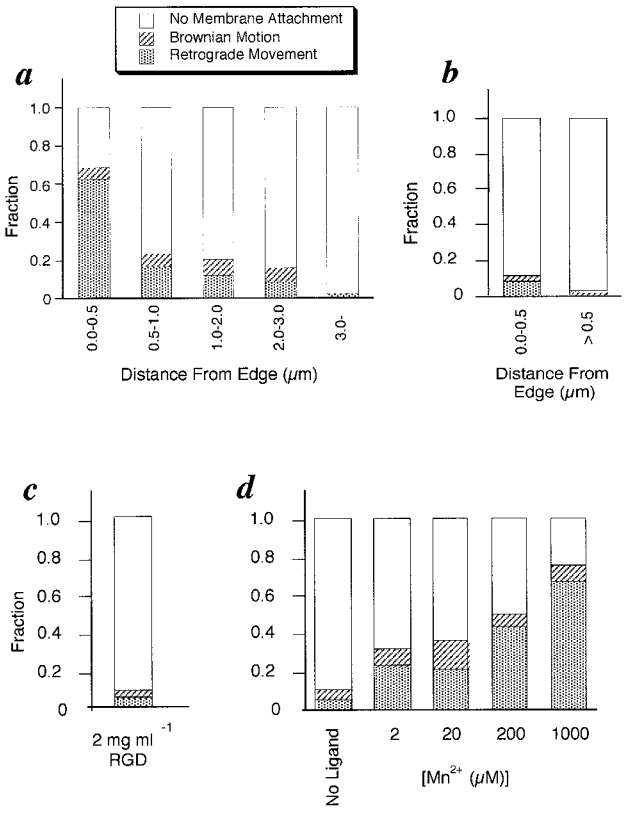

Fig. 2. Histograms are shown of the probability of bead binding. (*a*) The position dependence of beads coated with a low concentration of FNIII7–10 (total n = 272). At this concentration, we estimate that 300 FNIII7–10 molecules are bound per bead (4–10/bead-membrane contact area). (*b*) The control experiment for *a*. Beads were coated with 100% BSA (total n = 75) instead of FNIII7–10. (*c*) The same experiment as *a* in the presence of 2 mg/ml RGD peptide, which inhibits fibronectin binding to the β1 integrin (19, 20). This experiment was done within 0.5 μm from the edge (total n = 94). This result coincides with ref. 1. (*d*) Edge binding of FN beads is measured as a function of [Mn^{2+}], which is reported to change the affinity of integrin for fibronectin (20–22). The binding probability is dependent on the concentration of Mn^{2+} (total n = 252).

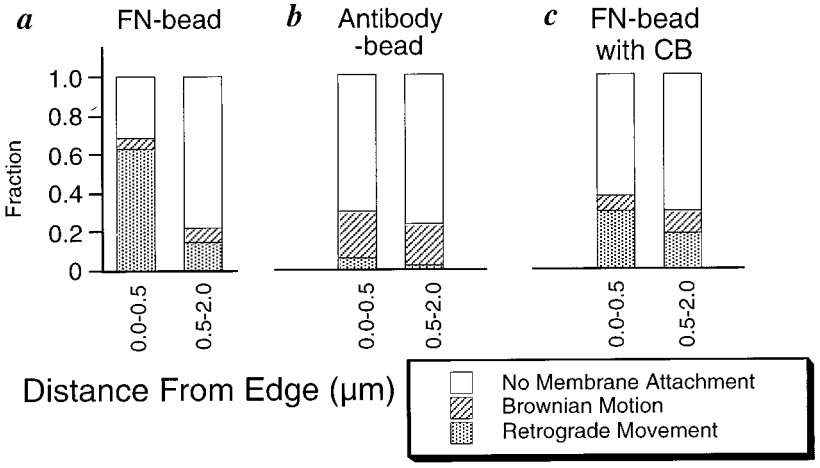

Fig. 3. (*a*, *b*, and *c*) Histograms of the bead binding behavior at the front part of migrating fibroblasts. (*a*) Fibronectin-coated bead. This histogram is based on the same set of data for Fig. 2*a*. (*b*) ES66 antibody-coated beads. (*c*) Fibronectin-coated beads in the presence of 100 nM cytochalasin B. For more details, see *Materials and Methods*.

beads coated with BSA and with no FNIII7–10 (Fig. 2*b*). The probability of the membrane attachment was greatly decreased at all positions on the lamellipodium. Second, we added RGD to compete for fibronectin binding to integrin (19, 20) and found that only 10% of the beads bound (Fig. 2*c*). These results indicate that the majority of the beads that we studied were attached in a ligand-specific manner. Third, we changed the concentration of divalent cations in the medium because the fibronectin–integrin interaction is divalent cation dependent (20–22). In low concentrations of manganese ion, spreading will occur on laminin but fibronectin–integrin binding is blocked (20). We measured the binding of fibronectin beads to cells spread on laminin, as a function of manganese ion. As shown in Fig. 2*d*, the membrane attachment of the fibronectin beads depends on the concentration of manganese (apparent K_d: 210 μM). A similar manganese ion concentration dependence has been reported for $\alpha5\beta1$ integrin–fibronectin binding (21). To further test whether or not $\alpha5\beta1$ integrin was the major fibronectin-binding site, we added an inhibiting anti-$\alpha5$ antibody before measuring fibronectin bead binding. Anti-$\alpha5$ antibody caused a 70 ± 5% decrease in binding both at the edge and back from the edge, whereas an anti-αv antibody only caused ≈15 ± 4% inhibition of fibronectin bead binding. Thus, we suggest that binding of the FNIII7–10 beads is primarily to $\alpha5\beta1$ integrin.

Distribution of $\beta1$ Integrin on the Cell Surface and the Contribution of Cytoskeleton to the Edge-Specific Binding. To determine whether the edge specificity simply reflects the concentration of the fibronectin receptor on the cell surface, we checked whether or not there was any evidence of a concentration of $\beta1$ integrin at the edge, using fluorescent antibody staining or antibody-coated beads. As was observed previously (23), we found that fluorescent anti-$\beta1$ antibody staining of the membranes did not show any edge concentration of $\beta1$. Surface carbohydrates could interfere with fibronectin bead as well as antibody bead binding but may not interfere with antibody binding alone. Thus, the distribution of antibody-coated bead binding controls for functional differences in bead binding as well as the distribution of integrin. Beads were coated with a nonperturbing antibody for chicken $\beta1$ integrin chain, ES66. The binding probability of the beads was checked on NIH 3T3 mouse fibroblasts transfected with chick $\beta1$ (7, 14). The lamellipodium was separated into two areas, within 0.5 μm and from 0.5 μm to 2.0 μm back from the leading edge, and compared with the results of fibronectin-coated bead binding to the equivalent cells (Fig. 3 *a* and *b*). There was no detectable position-dependent binding of ES66 beads (the difference in Fig. 3*b* is almost the same as the difference of the control experiment in Fig. 2*b*), and the probability of retrograde movement was decreased to the level of the control experiment (compare Fig. 2*b* with Fig. 3*b*). Only 3% of control antibody beads bound under these conditions and ES66 beads bound to the parent 3T3 cells (without chicken $\beta1$ integrin) at the control level (3%). In another experiment, a higher level of bead binding (43% at edge and 39% back from the edge) was obtained but again no positional difference was observed. These results indicate that the edge specific binding does not originate from the asymmetric distribution of $\alpha5\beta1$ integrin.

The contribution of cytoskeleton to the edge specific binding was studied by altering actin dynamics with cytochalasin B (5, 24). More than 0.5 μM of cytochalasin caused migrating fibroblasts to immediately become round and detach. This result suggested that the rigid cytoskeletal structure, which depended on receptor binding to ECM, is needed to keep the cells attached to the substrate. With moderate cytochalasin treatment (100 nM), the cells were still attached to the substrate. We then examined the edge specificity of FNIII7–10 bead binding (Fig. 3*c*) with and without cytochalasin. The edge-specific binding was decreased, even though retrograde movement did not disappear completely. No remarkable differences were observed in actin filament distribution as visualized by rhodamine-phalloidin with or without 100 nM cytochalasin (data are not shown). Thus, the edge specificity of binding is altered by altering actin dynamics.

Position Dependence of Release of Fibronectin-Coated Beads from the Cell Surface. After beads left the leading edge, we followed them until they stopped moving and in many cases (n = 22) released from the cell surface. Cessation of movement and release were position and not time dependent. The velocity of retrograde movement decreased and diffusive movement increased when the beads reached the endoplasm–ectoplasm boundary (at 95 s in Fig. 1*c* and >50% of beads started diffusing). Many of the diffusing beads (32% of total, n = 69) released completely (Fig. 1*a*, *iv–vi*). Nonspecific binding between the beads and the membrane may hinder the complete detachment of some of the beads, or multiple weak interactions could keep the beads attached for the observation period (1–2 min). BSA beads that were nonspecifically attached did not detach (data are not shown), indicating that the release of the bead involved specific integrin binding.

Two models for bead release were quantitatively tested, either time-dependent or position-dependent release. In Fig. 1*a*, the bead detached from the cell at the boundary between ectoplasm and endoplasm (see *Materials and Methods* for definition), which indicated that release was position specific. Alternatively, release could occur in a stochastic manner. If release was stochastic, the frequency of the release events should follow a single exponen-

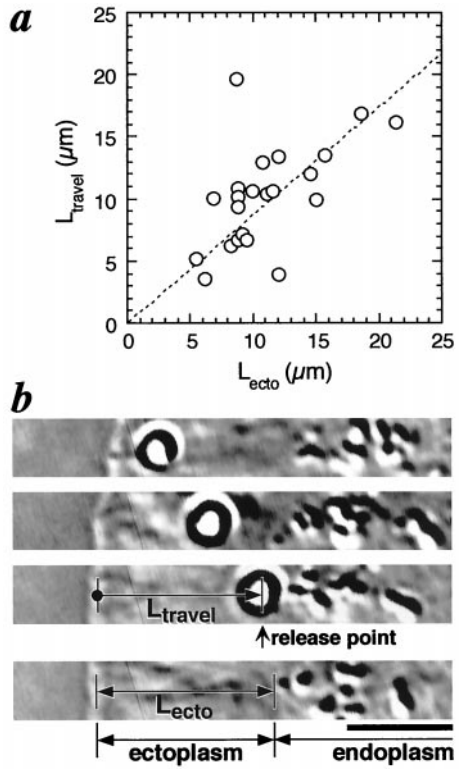

Fig. 4. (*a*) The position dependence of the unbinding of the beads from cell surfaces. The position where the unbinding of the bead occurred, indicated by the length of bead travel before unbinding (L_{travel}), is related to the position of the ectoplasm–endoplasm boundary, indicated by the length of ectoplasm (L_{ecto}). The dashed line is a linear approximation and the slope is 0.87. (*b*) Video micrographs show the definition of L_{travel} and L_{ecto} in *a*. The bead ceased moving rearward in the third micrograph and diffused away in the fourth micrograph. In micrographs (1–3), intervals are 21 s. (Scale bar, 5 μm).

tial decay (18, 25). However, the time dependence of release did not follow a single exponential decay (correlation coefficient r = 0.31, data are not shown). On the other hand, the position where the release occurred was related to the boundary between ectoplasm and endoplasm (r = 0.80, Fig. 4*a*). From these data, we conclude that release of the beads was not stochastic but was dependent on the position on the cell surface.

Discussion

We have found a position-dependent cycle of fibronectin–integrin–cytoskeleton binding, movement, and release. Fibronectin-coated beads bound preferentially within 0.5 microns of the leading edge to motile but not cytochalasin B-treated fibroblasts. When the beads were coated with a low density of fibronectin to reduce but not eliminate cooperative binding by multiple ligands, release of bead binding was found at the ectoplasm–endoplasm boundary. We hypothesize that this cycle of fibronectin binding, movement, and release is involved in cell motility.

The preferential edge binding is not explained by a simple binding mechanism. There is no preferential binding of anti-integrin antibody beads to the leading edge (Fig. 3*b*), and fluorescent anti-integrin antibody distribution shows no edge concentration. We have previously observed the preferential trapping of β1 integrin at the leading edge of these fibroblasts but that did not result in a concentration there, possibly because of the other factors causing depletion of integrins from the leading edge (14). In the fish keratocyte system, we have found an edge concentration of the β1 integrin that can explain some of the edge concentration of binding in that system. In the 3T3 fibroblast system, however, neither a concentration of active integrins at the leading edge nor a masking of bead binding back from the leading edge could explain edge specificity.

Differences in the avidity of binding caused by cytoskeletal linkage could explain the preference for binding at the leading edge. When ligands bind to receptors with low affinity, the presentation of multiple ligands on a bead greatly increases the avidity. A further increase in cooperativity may occur when the receptors are crosslinked by the cytoskeleton after ligand binding. Fibronectin binds weakly to integrins and an off-rate of 3 s has been measured with fibronectin-coated gold particles and soluble FNIII7–10 (D. Choquet and D. P. Felsenfeld, unpublished observations). Thus, multiple fibronectin-integrin bonds are needed for beads to remain bound for several minutes as observed and cytoskeletal crosslinking of the liganded integrins would greatly decrease the rate of release of beads from the membrane (Fig. 5).

Preferential binding to the cytoskeleton does occur at the edge of fish keratocytes (5) in the case of concanavalin A-coated beads. In the case of fibronectin-coated beads on 3T3 cells, attachment to the cytoskeleton occurs preferentially at the edge. The integrins appear unattached to cytoskeleton before ligand binding (1, 14). At intermediate anti-β1 antibody concentrations on the bead surface, the beads often diffused but would attach to the cytoskeleton if taken to the leading edge (D. Choquet and D. P. Felsenfeld, unpublished results). Fibronectin–integrin binding often produces cytoskeletal attachment of integrin (1, 16), but a larger fraction of beads diffused when bound away from the edge. In these experiments conditions were chosen to give a low level of binding on the lamellipodium (<30%). This level of binding enabled the definition of the most optimal binding location. An increased rate of cytoskeletal attachment of

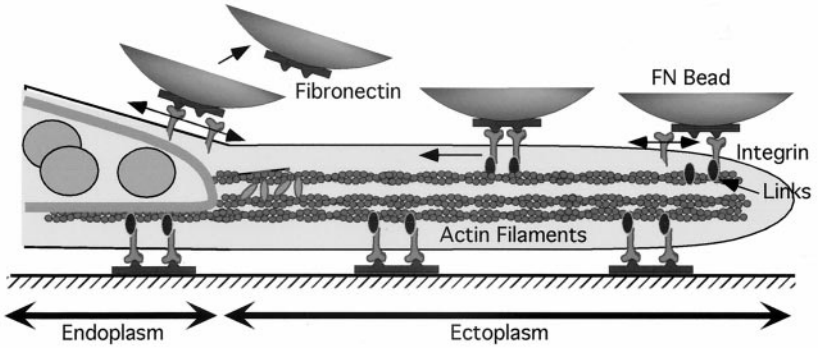

Fig. 5. Schematic illustration showing that cytoskeleton binding of integrin-fibronectin complexes at the leading edge could stabilize them. A fibronectin-coated bead (FN-bead) attaches to the dorsal surface of the leading edge and recruits a second integrin, which recruits a second link to the cytoskeleton. Because the two bound integrins are attached to a rigid cytoskeleton, they cannot diffuse away if one should release from the fibronectin. Therefore, bead binding is stabilized until the actin cytoskeleton depolymerizes, which is often seen at the endoplasm–ectoplasm boundary. Upon release from the cytoskeleton, the integrins could diffuse away leading to FN-bead release. On the ventral surface, additional components could stabilize the integrin-cytoskeleton complex perhaps in a force-dependent process (1). Such a position-dependent binding and release cycle could aid cell migration.

liganded integrins at the leading edge is consistent with other findings and could explain increased bead binding.

If crosslinking of liganded receptors caused increased edge binding, then the loss of cytoskeletal attachment at the ectoplasm–endoplasm boundary could explain the release of the beads at that point. All beads that released from the membrane started to diffuse laterally before they released. In other words, detachment of integrins from the cytoskeleton preceded the fibronectin bead release. There are three major alternative explanations for detachment of integrins from the cytoskeleton: i) a reversible biochemical process decreases the affinity of individual integrins for the cytoskeleton, ii) proteolysis of the integrins leads to detachment, or iii) depolymerization of actin filaments occurs in that region. The second possibility is less likely than others because of previous observations of integrin recycling (3, 11, 26, 27). Depolymerization of actin does occur at the ectoplasm–endoplasm boundary, and modification of the cytoplasmic tails of the integrins does modify their interactions with the forward transport system and with the cytoskeleton (14, 16). Both mechanisms, i and iii, could be involved in the dissociation of the liganded integrins from the cytoskeleton at the ectoplasm–endoplasm boundary.

Release of the beads from the membrane is potentially analogous to the release of a portion of the integrins from fibronectin surfaces. Both biochemical release and mechanical release have been postulated previously. In the case of the $\alpha v\beta 3$ integrin, there is evidence for cytoplasmic regulation of the integrin-matrix binding through the action of a calcium-dependent phosphatase (11). Mechanical dissociation of matrix linkages has been reported at the rear of cells (7, 8). If the binding of ligand stabilizes the conformation of an integrin, which has high affinity to the cytoskeleton, it is also possible that binding of the cytoskeleton stabilizes a high affinity conformation. Thus, both the bead release from the cytoskeleton and the release from the membrane can be coupled.

Here, we observed that the binding and some release of fibronectin molecules occurred in the front and the back of the endoplasmic region of the cell, respectively. In considering the bottom of the cell, the ventral integrins will perhaps show different position dependence because of reinforced integrin–fibronectin complexes (1) or the persistence of actin filaments at the lower surface. Some large aggregates persist from the front to the rear of the cell (7, 8). However, there is a major decrease in the area of contact of fibroblasts with the substratum from the front to the rear of the cell (trigonal shape) (7, 14). Furthermore, the force on ventral contacts switches direction near the nucleus or back from the endoplasm–ectoplasm boundary (2). These observations are consistent with the hypothesis that many integrin-ECM contacts are released near the nucleus of fibroblasts.

Models of cell migration have included a force generation step at the front of the cell that can be rate-limiting under certain conditions (see reviews in refs. 4, 28, and 29). Linkage between the force generating cytoskeleton and the fibronectin matrix could occur through cytoskeleton attachment of liganded integrins preferentially at the leading edge (see diagram in Fig. 5*a*). The rearward movement of the cytoskeleton would draw the cell forward. The release process could begin at the ectoplasm–endoplasm boundary as these findings show but may persist to the tail of the cell. Preferential attachment at the leading edge would enable the cell to pull for the maximal distance on the new ECM ligands that it encounters. In fan-shaped fish keratocytes, there is a very large lamellipodium that generates pulling forces on substrate contacts (C. G. Galbraith and M.P.S., unpublished observations; ref. 30), and the preferential attachment of crosslinked glycoproteins to the cytoskeleton at the edge has been observed as well (5). The finding of some release at the ectoplasm–endoplasm boundary indicates that a portion of integrins could recycle in front of the nucleus. Unliganded integrins can diffuse (16, 31) and single integrins and small aggregates move to the leading edge in the absence of bound ligand (14, 32). Such a surface transport mechanism could recycle integrins to the front of the lamellipodium. The alternative mechanism of endocytosis and transport back to the front of the cell by intracellular vesicles (3, 11, 26, 27) is unlikely because there are few intracellular microtubules in the lamellipodium. Thus, we hypothesize that cytoskeleton binding of liganded integrins stabilizes integrin–ligand complexes at the leading edge. Integrin release from the cytoskeleton would then shorten the lifetime of integrin–ligand bonds by allowing integrins to diffuse away from ECM ligands upon unbinding.

We thank H. P. Erickson for providing the recombinant FNIII7–10 and advice. The software and system for the bead trajectory analysis were developed by K. Kinosita, Jr. We thank D. Choquet, D. P. Felsenfeld, C. G. Galbraith, and D. Raucher for helpful comments on this work in progress. We also thank A. F. Horwitz for the cell line and K. M. Yamada for the hybridoma, ES66. T.N. was a recipient of a Japan Society for the Promotion of Science Fellowship for Japanese Junior Scientists during this work. This work was partly supported by a National Institutes of Health grant to M.P.S.

1. Choquet, D., Felsenfeld, D. P. & Sheetz, M. P. (1997) *Cell* **88,** 39–48.
2. Galbraith, C. G. & Sheetz, M. P. (1997) *Proc. Natl. Acad. Sci. USA* **94,** 9114–9118.
3. Bretscher, M. S. (1992) *EMBO J.* **11,** 405–410.
4. Sheetz, M. P., Felsenfeld, D. P. & Galbraith, C. G. (1998) *Trends Cell Biol.* **8,** 51–54.
5. Kucik, D. F., Kuo, S. C., Elson, E. L. & Sheetz, M. P. (1991) *J. Cell Biol.* **114,** 1029–1036.
6. Symons, M. H. & Mitchison, T. J. (1991) *J. Cell Biol.* **114,** 503–513.
7. Regen, C. M. & Horwitz, A. F. (1992) *J. Cell Biol.* **119,** 1347–1359.
8. Palecek, S. P., Schmidt, C. E., Lauffenburger, D. A. & Horwitz, A. F. (1996) *J. Cell Sci.* **109,** 941–952.
9. Palecek, S. P., Huttenlocher, A., Horwitz, A. F. & Lauffenburger, D. A. (1998) *J. Cell Sci.* **111,** 929–940.
10. Huttenlocher, A., Palecek, S. P., Lu, Q., Zhang, W., Mellgren, R. L., Lauffenburger, D. A., Ginsberg, M. H. & Horwitz, A. F. (1997) *J. Biol. Chem.* **272,** 32719–32722.
11. Lawson, M. A. & Maxfield, F. R. (1995) *Nature (London)* **377,** 75–79.
12. Leahy, D. J., Aukhil, I. & Erickson, H. P. (1996) *Cell* **84,** 155–164.
13. Suzuki, N., Miyata, H., Ishiwata, S. & Kinosita, K., Jr. (1996) *Biophys. J.* **70,** 401–408.
14. Schmidt, C. E., Horwitz, A. F., Lauffenburger, D. A. & Sheetz, M. P. (1993) *J. Cell Biol.* **123,** 977–991.
15. Reszka, A. A., Hayashi, Y. & Horwitz, A. F. (1992) *J. Cell Biol.* **117,** 1321–1330.
16. Felsenfeld, D. P., Choquet, D. & Sheetz, M. P. (1996) *Nature (London)* **383,** 438–440.
17. Gelles, J., Schnapp, B. J. & Sheetz, M. P. (1988) *Nature (London)* **331,** 450–453.
18. Nishizaka, T., Miyata, H., Yoshikawa, H., Ishiwata, S. & Kinosita, K., Jr. (1995) *Nature (London)* **377,** 251–254.
19. Gehlsen, K. R., Argraves, W. S., Pierschbacher, M. D. & Ruoslahti, E. (1988) *J. Cell Biol.* **106,** 925–930.
20. Elices, M. J., Urry, L. A. & Hemler, M. E. (1991) *J. Cell Biol.* **112,** 169–181.
21. Gailit, J. & Ruoslahti, E. (1988) *J. Biol. Chem.* **263,** 12927–12932.
22. Lange, T. S., Bielinsky, A. K., Kirchberg, K., Bank, I., Herrmann, K., Krieg, T. & Scharffetter-Kochanek, K. (1994) *Exp. Cell Res.* **214,** 381–388.
23. Felsenfeld, D. P., Schwartzberg, P. L., Venegas, A., Tse, R. & Sheetz, M. P. (1999) *Nat. Cell Biol.* **1,** 200–206.
24. Forscher, P. & Smith, S. J. (1988) *J. Cell Biol.* **107,** 1505–1516.
25. Erickson, H. P. (1994) *Proc. Natl. Acad. Sci. USA* **91,** 10114–10118.
26. Bretscher, M. S. (1989) *EMBO J.* **8,** 1341–1348.
27. Sczekan, M. M. & Juliano, R. L. (1990) *J. Cell. Physiol.* **142,** 574–580.
28. Lauffenburger, D. A. & Horwitz, A. F. (1996) *Cell* **84,** 359–369.
29. Mitchison, T. J. (1996) *Cell* **84,** 371–379.
30. Oliver, T., Dembo, M. & Jacobson, K. (1999) *J. Cell Biol.* **145,** 589–604.
31. Yauch, R. L., Felsenfeld, D. P., Kraeft, S. K., Chen, L. B., Sheetz, M. P. & Hemler, M. E. (1997) *J. Exp. Med.* **186,** 1347–1355.
32. Kucik, D. F., Elson, E. L. & Sheetz, M. P. (1989) *Nature (London)* **340,** 315–317.